

MEASUREMENTS OF COSMIC-RAY ELECTRONS AND POSITRONS BY THE WIZARD/CAPRICE COLLABORATION

M. Boezio¹, G. Barbiellini¹, V. Bonvicini¹, P. Schiavon¹, A. Vacchi¹, N. Zampa¹, D. Bergström², P. Carlson², T. Francke², S. Grinstein², N. Weber², M. Suffert³, M. Hof⁴, J. Kremer⁴, W. Menn⁴, M. Simon⁴, S.A. Stephens⁵, M. Ambriola⁶, R. Bellotti⁶, F. S. Cafagna⁶, F. Ciacio⁶, M. Circella⁶, C. De Marzo⁶, N. Finetti⁷, P. Papini⁷, S. Piccardi⁷, P. Spillantini⁷, S. Bartalucci⁸, M. Ricci⁸, C. Grimani⁹, M. Casolino¹⁰, M.P. De Pascale¹⁰, A. Morselli¹⁰, P. Picozza¹⁰, R. Sparvoli¹⁰, J.W. Mitchell¹¹, J.F. Ormes¹¹, R.E. Streitmatter¹¹, U. Bravar¹², and S.J. Stochaj¹²

¹Dipartimento di Fisica dell'Università and Sezione INFN di Trieste, Via A. Valerio 2, I-34147 Trieste, Italy

²Royal Institute of Technology (KTH), S-104 05 Stockholm, Sweden

³Centre des Recherches Nucléaires, BP20, F-67037 Strasbourg-Cedex, France

⁴Universität Siegen, 57068 Siegen, Germany

⁵Tata Institute of Fundamental Research, Bombay 400 005, India

⁶Dipartimento di Fisica dell'Università and Sezione INFN di Bari, Via Amendola 173, I-70126 Bari, Italy

⁷Dipartimento di Fisica dell'Università and Sezione INFN di Firenze, Largo Enrico Fermi 2, I-50125 Firenze, Italy

⁸Laboratori Nazionali INFN, Via Enrico Fermi 40, CP 13, I-00044 Frascati, Italy

⁹Istituto di Fisica dell'Università di Urbino, Urbino, Italy

¹⁰Dipartimento di Fisica dell'Università and Sezione INFN di Roma, Tor Vergata, Via della Ricerca Scientifica 1, I-00133 Roma, Italy

¹¹Code 661, NASA/Goddard Space Flight Center, Greenbelt, MD 20771, USA

¹²Box 3-PAL, New Mexico State University, Las Cruces, NM 88003, USA

ABSTRACT

Two recent balloon-borne experiments have been performed by the WiZard/CAPRICE collaboration in order to study the electron and positron components in the cosmic radiation.

In 1994 August 8-9 the CAPRICE94 experiment flew from northern Canada and on 1998 May 28-29 the CAPRICE98 experiment flew from New Mexico, USA at altitudes corresponding to 3.9 and 5.5 g/cm² of average residual atmosphere respectively. The apparatus were equipped with a Ring Imaging Cherenkov (RICH) detector, a time-of-flight system, a superconducting magnet spectrometer with a tracking system and a 7-radiation-length silicon-tungsten imaging calorimeter. The RICH used in 1994 had a solid NaF radiator while in 1998 the RICH had a C₄F₁₀ gaseous radiator.

We report on the electron and positron spectra and positron fraction at the top of the atmosphere from few hundred MeV to 40 GeV measured by these two experiments.

© 2001 COSPAR. Published by Elsevier Science Ltd. All rights reserved.

INTRODUCTION

Precise measurements of the electron component of the cosmic radiation provide important information about the propagation of the cosmic rays in the Galaxy which is not accessible from the study of cosmic-ray nuclear components. In fact, because of their low mass, electrons undergo severe energy loss through bremsstrahlung and synchrotron radiation in the magnetic field and inverse Compton scattering with the ambient photons.

Along with the measurements of electrons, the study of the cosmic-ray positrons, which are believed to be

mostly produced in collisions of cosmic-ray nucleons with interstellar matter, provide additional information on propagation models. Furthermore, production mechanism and other possible new sources of positrons can be investigated.

Since the first detections of electrons and positrons in the early sixties, many experiments were performed to measure these components. Their results, however, show large discrepancies and discordant conclusions have been drawn (e.g. see Müller, 1995). In recent years a new generation of experiments with more sophisticated detectors have been performed and their results are in much better agreement (Golden et al., 1994; Barwick et al., 1997; Barwick et al., 1998; Boezio et al., 2000). In this paper we present the results on the cosmic-ray electron and positron spectra and ratios obtained with the NMSU-WIZARD/CAPRICE balloon-borne spectrometer, which flew in 1994 and 1998.

DETECTOR SYSTEM

The first version of the apparatus, called CAPRICE94, was launched from Lynn Lake, Manitoba, Canada on August 8th, 1994 and it landed near Peace River, Alberta, Canada. The balloon floated at an average atmospheric depth of 3.9 g/cm^2 for nearly 23 hours at a mean vertical cutoff rigidity of about 0.5 GV/c .

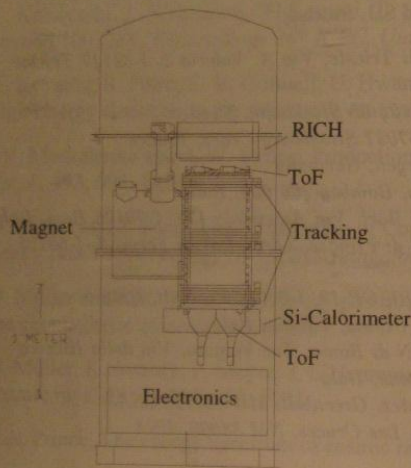


Fig. 1. Schematic view of the CAPRICE94 apparatus.

The instrument (Figure 1) included from top to bottom a Ring Imaging Cherenkov (RICH) detector with a solid NaF radiator having a threshold Lorentz factor of 1.5 (Carlson et al., 1994), a time-of-flight system (ToF), a superconducting magnet spectrometer with a tracking system made by a stack of multiple proportional chambers (MWPC) (Golden et al., 1991) and two drift chambers (Hof et al., 1994), and a 7-radiation-length silicon-tungsten imaging calorimeter (Boccolini et al., 1996). The average maximum detectable rigidity (MDR) of this spectrometer was 175 GV/c .

The second version of the instrument (Figure 2), hereafter called CAPRICE98, was launched from Escondido, Summer, New Mexico, on 28th May 1998. It floated at an average atmospheric depth of 5.5 g/cm^2 for a period of 21h at a mean vertical cutoff rigidity of about 4.5 GV/c and it landed close to Heber, Arizona. In this experiment the MWPCs in the CAPRICE94 apparatus were replaced by an additional drift chamber providing an MDR of 330 GV/c and the RICH used a C_4F_{10} gaseous radiator with a threshold Lorentz factor of about 19 (Francke et al., 1999).

DATA ANALYSIS

The CAPRICE experiments were well suited for the identification of cosmic-ray electrons and positrons and the reconstruction of their energy spectra. The combined capabilities of the RICH and calorimeter also

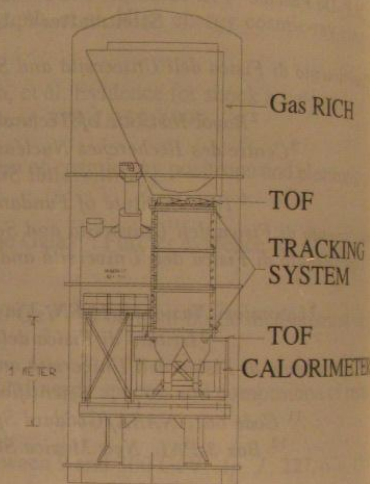


Fig. 2. Schematic view of the CAPRICE98 apparatus.

with the time-of-flight and pions and positrons than 10^5 was achieved by distinguishing different components of the rigidity dependence of the precise determination.

Fig. 3. Display of CAPRICE98 instruments. The RICH and calorimeter are shown the RICH and calorimeter also from above. No hits are shown in the calorimeter e.g. the calorimeter shown in the figure indicate hits and the drift time. The drift time (x) is to the left of the calorimeter right. The calorimeter shows the magnetic shower into

Above the RICH detector the CAPRICE98 experiment wider rigidity range detected per ring of about 10^{-4} up to 10^4 GV/c . The remaining magnetic showers in the calorimeter and singly charged particles are strong ionizations are strong 10^4 , with an efficiency of the gas-RICH in the Muons and pions. Figures 4 (b) a

...the time-of-flight information permitted the identification of electrons against a background of muons and positrons against a vast background of protons, muons and pions. A rejection factor of better than 10^5 was achieved in both experiments for protons against positrons. Furthermore, the capability of distinguishing different particles independently with the different detectors allowed a reliable determination of the rigidity dependent efficiency and rejection power of each individual detector, which was essential for a precise determination of the energy spectra.

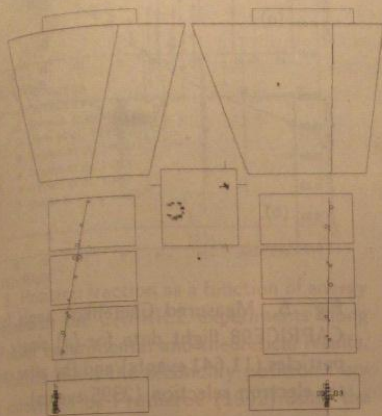


Fig. 3. Display of a 6.7 GeV/c electron in the CAPRICE98 instrument. From top to bottom are shown the RICH from the side (in the center also from above), the tracking system, and the calorimeter. Note that the figure is not to scale, e.g. the calorimeter is significantly thinner than shown in the figure. The circles in the DCs indicate hits and their radius is proportional to the drift time. The view of maximum bending (x) is to the left and the orthogonal (y) to the right. The calorimeter shows the electromagnetic shower induced by the electron.

Above the RICH threshold, the contamination slowly increased to 2% at 3 GV/c, and then to 30% at 5 GV/c and 60% at 5 GV/c. Above this rigidity protons became indistinguishable from positrons. In the CAPRICE98 experiments, the higher threshold of the gas-RICH permitted the selection of positrons in a wider rigidity range. The excellent imaging capabilities of the gas-RICH (on average 12 photoelectrons were detected per ring (Bergström et al., 1999)) permitted the selection of positrons with a proton contamination of about 10^{-4} up to 19 GV/c, increasing to about 1% at 30 GV/c.

The remaining proton rejection factor was provided by the calorimeter. Conditions to select electromagnetic showers in the calorimeter were based on the total detected energy, which should match the measured momentum, and on the longitudinal and lateral profiles of the shower. Figures 4 (b) and 5 (b) show the singly charged sample after the electron calorimeter selection. Both the proton and the muon/pion contaminations are strongly reduced. The calorimeter criteria were chosen to provide a rejection factor of about 10^3 , with an efficiency of about 85%, in CAPRICE94 and, because of the high identification capability of the gas-RICH in a wider rigidity range, of about 10^3 , with an efficiency higher than 90%, in CAPRICE98. Muons and pions were efficiently rejected by the calorimeter (Boezio et al., 2000).

Figures 4 (b) and 5 (b) clearly show that the combined calorimeter and RICH selections provide a clean

In both experiments, singly charged particles moving downward were selected using the time-of-flight and tracking information. The selection of electrons and positrons in a background of singly charged particles was performed using the RICH and the calorimeter. Figure 3 shows the display of an identified 6.7 GeV electron from the CAPRICE98 flight data. The response of each detector can be seen.

In both experiments electrons were selected with a rigidity at the spectrometer between 0.3 and 30 GV/c. In CAPRICE94 positrons were identified between 0.3 and 10 GV/c, while in CAPRICE98 between 0.3 and 30 GV/c. The different rigidity range for the positron selection was due to the different refractive index of the radiator for the two RICH detectors. This can be seen in Figures 4 and 5 which show the measured Cherenkov angle for singly charged particles as a function of rigidity for the CAPRICE94 and the CAPRICE98 experiment respectively. In the NaF RICH (Figure 4), due to the lower threshold, a good positron to proton separation was achieved up to 5 GV/c. The proton contamination in the RICH selection was found to be less than 0.1% up to 1.2 GV/c where protons were below the RICH threshold.

identification of the electron and positrons.

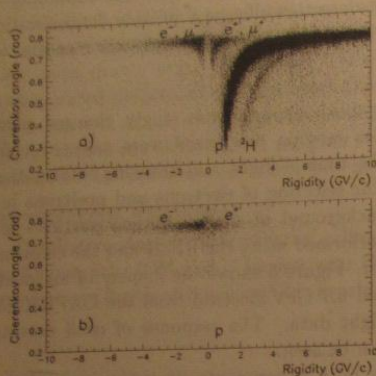


Fig. 4. Measured Cherenkov angle from the CAPRICE94 flight data for (a) singly charged particles (356,127 events) and (b) after calorimeter electron selection (5087 events).

RESULTS

The observed number of electrons and positrons were corrected for the selection efficiencies and geometric factors. The resulting differential spectra were extrapolated to the top of the payload using bremsstrahlung corrections. From these spectra we subtracted the atmospheric secondary electron and positron fluxes, and the theoretical estimates given by Stephens (1981).

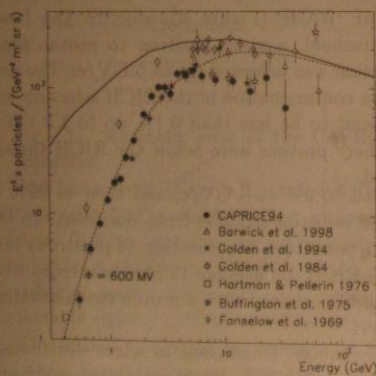


Fig. 6. The electron spectrum for CAPRICE94 compared with other experimental results. The solid line is a prediction by Moskalenko and Strong (1998). The dashed line is the same spectrum modulated using a spherically symmetric model with solar modulation parameter $\phi = 600$ MV.

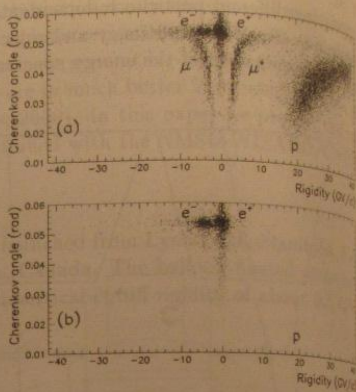


Fig. 5. Measured Cherenkov angle from the CAPRICE98 flight data for (a) singly charged particles (11,641 events) and (b) after calorimeter electron selection (2395 events).

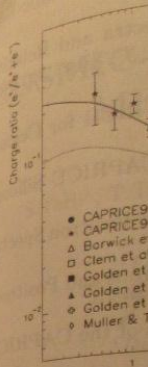


Fig. 8. Positron spectrum measured by the CAPRICE94 compared with other experimental results. The dotted line is the calculated leaky-box model positron fraction from Strong (1998).

Also a good agreement is seen with the prediction of Moskalenko and Strong (1998). In this case the CAPRICE94 data are in good agreement with the determined solar modulation parameter. It is worth noting that all positrons were measured in the CAPRICE94 payload. A similar conclusion can be drawn from the theoretical prediction of Moskalenko and Strong (1998) using the CAPRICE data of Couto et al. (1999) and the positron measurements of

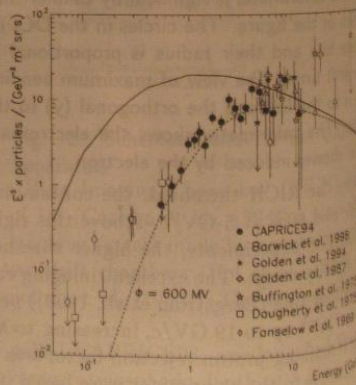


Fig. 7. The positron spectrum for CAPRICE94 compared with other experimental results. The solid line is the calculated interstellar secondary positron spectrum (Moskalenko and Strong 1998). The dashed line is the same spectrum modulated using a spherically symmetric model with solar modulation parameter $\phi = 600$ MV.

ACKNOWLEDGMENTS

This work was supported by the Agenzia Spaziale Italiana, the Swedish Space Board, the Swedish Space Foundation. We would like to thank Lynn Lake and

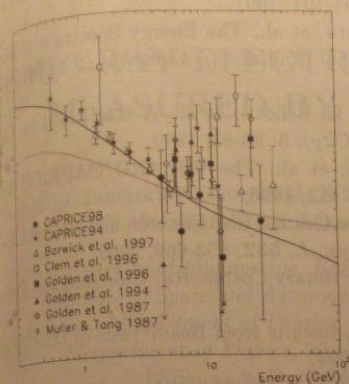


Fig. 8. Positron fraction as a function of energy measured by the CAPRICE experiments along with other experimental and theoretical results. The dotted line is the secondary positron fraction calculated by Protheroe (1992) using the leaky-box model. The solid line is the secondary positron fraction calculated by Moskalenko and Strong (1998).

Also a good agreement at low energies (below about 6 GeV) can be seen between the CAPRICE94 results with the prediction of Moskalenko and Strong (1998) modulated using a spherically symmetric model with solar modulation parameter $\phi = 600$ MV. At high energies, the theoretical electron spectrum is higher than CAPRICE94 results which could indicate that the injection spectrum is steeper than the one used by Moskalenko and Strong (1998). The data can also be reconciled if a lower normalization would be used for the calculated spectrum (obtained from experimental data by Moskalenko and Strong, 1998). However, in this case the CAPRICE94 data at low energy either would indicate a steeper electron interstellar spectrum than determined by Moskalenko and Strong (1998) or would not agree with a spherical symmetric model for solar modulation.

It is worth noticing that the positron spectrum was calculated by Moskalenko and Strong (1998) assuming that all positrons were of secondary origin, produced by the interaction of cosmic-ray nuclei with interstellar matter. The CAPRICE results are in agreement with a pure secondary origin of the positron component.

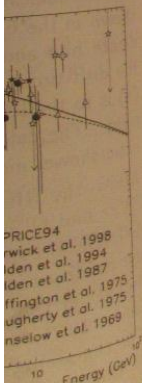
A similar conclusion can be drawn from the CAPRICE results on the positron fraction. Figure 8 shows the positron fraction measured in the two CAPRICE experiments along with other experimental results and theoretical predictions (Protheroe, 1982, Moskalenko and Strong, 1998) for positron secondary production. CAPRICE data do not confirm the possible indication of a primary component near 10 GeV claimed by Costa et al. (1999). However, the data are statistically limited. It is essential to improve the statistics on positron measurements in the high energy region.

ACKNOWLEDGEMENTS

This work was supported by NASA Grant NAGW-110, The Istituto Nazionale di Fisica Nucleare, Italy, the Agenzia Spaziale Italiana, DARA and DFG in Germany, EU SCIENCE, the Swedish National Space Board, the Swedish Council for Planning and Coordination of Research and the Knut and Alice Wallenberg Foundation. We wish to thank the National Scientific Balloon Facility and the NSBF launch crew that served in Lynn Lake and Fort Sumner.

The corrected electron and positron spectra were propagated backward to the top of the atmosphere by simultaneously solving the cascade equations, which describe the propagation of all the electromagnetic components, namely, primary electrons, positrons and secondary gamma rays that result from bremsstrahlung of the electron component. From this, we obtained the electron and positron spectra which are shown together with other experimental results and theoretical predictions in Figures 6 and 7, respectively. A good agreement is found between the CAPRICE94 electron spectrum and the recent results by Golden et al. (1994) and between the CAPRICE94 positron spectrum and the data by HEAT94 (Barwick et al., 1998). Instead, the HEAT94 electron flux is about 70% higher than CAPRICE94 results. It is worth pointing out that a 20% systematic uncertainty in the energy estimation can explain this difference. Furthermore, the combined HEAT94 and HEAT95 electron results from 1 to 50 GeV (Du Vernois et al., 1999) on the electron spectrum are in better agreement with CAPRICE94 data.

angle from the singly charged after calorimetry). and geometrical bremsstrahlung electron fluxes, using



um for CAPRICE94 experimental results. The interstellar secondary positron fraction calculated by Moskalenko and Strong (1998) using a spherically symmetric model with solar modulation parameter $\phi = 600$ MV.

REFERENCES

- Barwick, S.W., J. J. Beatty, A. Bhattacharyya, C. R. Bower, C. J. Chaput, Measurements of the Cosmic-Ray Positron Fraction from 1 to 50 GeV, *Astrophys. J.*, **482**, L191-194, 1997.
- Barwick, S.W., J.J. Beatty, C.R. Bower, C.J. Chaput, S. Coutu, et al., The Energy Spectra and Relative Abundances of Electrons and Positrons in the Galactic Cosmic Radiation, *Astrophys. J.*, **498**, 770-780, 1998.
- Bergström, D., M. L. Ambriola, G. Barbiellini, S. Bartalucci, R. Bellotti, et al., A Gas RICH for Cosmic-Ray Studies, *Proc. 26th Int. Cosmic Ray Conf. (Salt Lake City)*, **5**, 80-83, 1999.
- Bocciolini, M., F. Celletti, N. Finetti, M. Grandi, P. Papini, et al., The WIZARD/CAPRICE Silicon Tungsten Calorimeter, *Nucl. Instr. and Meth.*, bf A370, 403-412, 1996.
- Boezio, M., P. Carlson, T. Francke, N. Weber, M. Hof, et al., The Cosmic-Ray Electron and Positron Spectrum Measured at 1 AU During Solar Minimum Activity, *Astrophys. J.*, **532**, 653-669, 2000.
- Buffington, A., C. D. Orth, and G. F. Smooth, Measurement of Primary Cosmic-Ray Electrons and Positrons from 4 to 50 GeV, *Astrophys. J.*, **199**, 669-679, 1975.
- Carlson, P., T. Francke, S. Loeffgren, N. Weber, and M. Suffert, Results from Beam Tests of the CAPRICE RICH Detector, *Nucl. Instr. and Meth.*, bf A349, 577-591, 1994.
- Clem, J. M., D. P. Clements, J. Esposito, P. Evenson, D. Huber, et al., Solar Modulation of Cosmic Electron and Positron Spectra, *Astrophys. J.*, **464**, 507-515, 1996.
- Coutu, S., S. W. Barwick, J. J. Beatty, A. Bhattacharyya, C. R. Bower, et al., Cosmic-Ray Positrons: Are There Primary Sources?, *Astropart. Phys.*, **11**, 429-435, 1999.
- Daugherty, J. K., R. C. Hartman, and P. J. Schmidt, A Measurement of Cosmic-Ray Positron and Negatron Spectra Between 50 and 800 MV, *Astrophys. J.*, **198**, 493-505, 1975.
- Du Vernois, M. A., S. W. Barwick, J. J. Beatty, A. Bhattacharyya, C. R. Bower, et al., Electron and Positron Energy Spectra: HEAT magnet spectrometer results, *Proc. 26th Int. Cosmic Ray Conf. (Salt Lake City)*, **3**, 49-52, 1999.
- Fanselow, J. L., R. C. Hartman, R. H. Hildebrand, and P. Meyer, Charge Composition and Energy Spectra of Primary Cosmic-Ray Electrons, *Astrophys. J.*, **158**, 771-780, 1969.
- Francke, T., D. Bergström, M. Boezio, P. Carlson, and M. Suffert, A Gas-RICH Detector for Space, *Nucl. Instr. and Meth.*, **A433**, 87-91, 1999.
- Golden, R. L., B.G. Mauger, G.D. Badhwar, R.R. Daniel, J.L. Lacy, et al., A Measurement of the Absolute Flux of Cosmic Ray Electrons, *Astrophys. J.*, **287**, 622-632, 1984.
- Golden, R. L., B. G. Mauger, S. Horan, S. A. Stephens, R. R. Daniel, et al., Observation of Cosmic-Ray Positrons in the Region from 5 to 50 GeV, *Astronomy and Astrophysics*, **188**, 145-154, 1987.
- Golden, R. L., C. Grimani, R. Hull, B.L. Kimbell, R. Park, et al., Performance of a Balloon-Borne Magnet Spectrometer for Cosmic Ray Studies, *Nucl. Instr. and Meth.*, **A306**, 366-377, 1991.
- Golden, R. L., C. Grimani, B. L. Kimbell, S. A. Stephens, S. J. Stochaj, et al., Observations of Cosmic-Ray Electrons and Positrons Using an Imaging Calorimeter, *Astrophys. J.*, **436**, 769-775, 1994.
- Golden, R. L., S. J. Stochaj, S. A. Stephens, F. Aversa, G. Barbiellini, et al., Measurement of the Positron to Electron Ratio in Cosmic Rays above 5 GeV, *Astrophys. J.*, **457**, L103-L106, 1996.
- Hartman, R. C., and C. J. Pellerin, Cosmic-ray Positron and Negatron Spectra Between 20 and 800 MV Measured in 1974, *Astrophys. J.*, **204**, 927-933, 1976.
- Hof, M., M. Bremerich, W. Menn, C. Pfeifer, O. Reimer, et al., Performance of Drift Chambers in a Magnet Rigidity Spectrometer for Measuring the Cosmic Radiation, *Nucl. Instr. and Meth.*, **A345**, 561-568, 1994.
- Moskalenko, V., and A. W. Strong, Production and Propagation of Cosmic-Ray Positrons and Electrons, *Astrophys. J.*, **493**, 694-707, 1998.
- Müller, D., and K. K. Tang, Cosmic-Ray Positrons from 10 to 20 GeV: a Balloon-Borne Measurement of the Geomagnetic East-West Asymmetry, *Astrophys. J.*, **312**, 183-194, 1987.
- Müller, D., The Cosmic Positron Fraction: Implications of a New Measurement, *Proc. 24th Int. Cosmic Ray Conf. (Rome)*, **3**, 13-16, 1995.
- Protheroe, R. J., On the Nature of the Cosmic Ray Positron Spectrum, *Astrophys. J.*, **254**, 391-397, 1986.
- Stephens, S. A., Secondary Components of Cosmic Radiation at Small Atmospheric Depths, *Proc. 26th Int. Cosmic Ray Conf. (Paris)*, **4**, 282-285, 1981.

New measurement
electron telescope
scintillating-fiber
of the background
with high granula
reported by the
best fit is obtain
once per 30 year

INTRODUCT

Major purpose
propagation pro
precise spectrum
compared with
questions, such
cosmic-ray prop

During propaga
by synchrotron
photon field. Th
in proportion to
the propagation

In order to cla
carried out by
Nishimura et al
the other compo

aspects were de
However, the
The reason the
during last ~ 30
at high energies